LIN28 expression and function in medulloblastoma

Ahmed Maklad
University of Tasmania
Mohammed Sedeeq
University of Tasmania
Richard Wilson
University of Tasmania
John A. Heath
Royal Hobart Hospital
Nuri Gueven
University of Tasmania
Iman Azimi (iman.azimi@utas.edu.au)
University of Tasmania

Research Article

Keywords: Medulloblastoma, LIN28A, LIN28B, Biomarker, Proliferation, Stemness

Posted Date: May 31st, 2022

DOI: https://doi.org/10.21203/rs.3.rs-1671258/v1

Abstract

Purpose Medulloblastoma (MB) is the most common malignant paediatric brain tumour. Current treatment modalities are not completely effective and can lead to severe neurological and cognitive adverse effects. In addition to urgently needing better treatment approaches, new diagnostic and prognostic biomarkers are required to improve the therapy outcomes of MB patients. The RNA binding proteins, LIN28A and LIN28B, are known to regulate invasive phenotypes in many different cancer types. However, the expression and function of these proteins in MB had not been studied to date.

Methods This study identified the expression of LIN28A and LIN28B in MB patient samples and cell lines and assessed the effect of LIN28 inhibition on MB cell growth, metabolism and stemness.

Results LIN28B expression was significantly upregulated in MB tissues compared to normal brain tissues. This upregulation, which was not observed in other brain tumours, was specific for the aggressive MB subgroups and correlated with patient survival and metastasis rates. Functionally, pharmacological inhibition of LIN28 activity concentration dependently reduced LIN28B expression, as well as the growth of D283 MB cells. While, LIN28 inhibition did not affect the levels of intracellular ATP, it reduced the expression of the stemness marker CD133 in D283 cells, and sphere formation of CHLA-01R cells. LIN28B, which is highly expressed in human cerebellum during the first few months after birth, subsequently decreased with age.

Conclusion The results of this study highlight the potential of LIN28B as a diagnostic and prognostic marker for MB and opens the possibility to utilise LIN28 as a pharmacological target to suppress MB cell growth and stemness.

1 Introduction

Medulloblastoma (MB) is an embryonal, malignant, cerebellar brain tumour, considered the most common and fast-growing primary paediatric brain tumour [1–3]. MB represents 20% of all childhood brain malignancies [3]. Based on the expression of specific genes, MB is classified into four subgroups (WNT, SHH, Group 3 and Group 4), which are further sub-classed into α, β, γ and δ subtypes by their molecular aetiology [4, 5]. Group 3 and Group 4 are characterised by higher rates of metastasis, lower survival and poorer prognosis compared to the other two MB subgroups [5, 6]. Current MB treatments include surgery, radiotherapy and chemotherapy, which are frequently combined to maximise treatment efficacy [2]. However, due to the harsh nature of the current treatments, surviving children often suffer from long-term neurological adverse effects [7, 8]. In addition, in about half of the children treated with chemotherapy alone (generally those less than 4 years of age), MB reoccurs [2]. Therefore, new therapeutic options are urgently needed to treat MB.

LIN28A (also known as LIN28) and its mammalian homologue LIN28B, are highly conserved RNA binding proteins [9, 10]. LIN28A was first discovered in *Caenorhabditis elegans* to regulate embryonic developmental timing [11, 12], while LIN28B was subsequently discovered in hepatocellular carcinoma

(HCC) [10]. Under physiological conditions, LIN28A and LIN28B regulate significant processes, such as tissue development including skeletal myogenesis, development of germ cells and neurogenesis as well as metabolism and pluripotency of embryonic stem cells [12–16]. LIN28A and B also have been implicated in pathophysiological conditions such as sickle cell disease, cardiac hypertrophy, diabetes, obesity, and cancer [14, 17–19]. Overexpression of LIN28A or LIN28B was associated with more aggressive tumours and poorer prognosis for many malignancies such as oesophageal cancer [20], hepatocellular carcinoma [10, 21], breast cancer [22, 23], germ cell tumours [14, 24–26], colon cancer [27, 28], ovarian cancer [29–31], gastric carcinoma [32, 33] as well as common paediatric tumours such as acute and chronic myeloid leukemia (AML and CML) [34, 35], Wilms tumour [36] and neuroblastoma [37]. Furthermore, some recent studies have revealed the role of LIN28A and/or B in cell proliferation, migration, invasion, metabolism and stemness in CNS tumours such as gliomas (especially glioblastoma) [38–40], embryonal tumours with multilayered rosettes (ETMRs) [41, 42], and atypical teratoid rhabdoid tumour (AT/RT) [43, 44]. However, expression and function of LIN28A and B in CNS cancer is still an emerging area of research.

Although the physiological importance of LIN28A and LIN28B in tissue regeneration and pluripotency in embryonal stem cells is well established, both genes have not been studied in MB. Therefore, this study systematically investigated expression of LIN28A and LIN28B in the different molecular MB subgroups and other brain tumours and correlated expression levels with tumour metastasis and patient survival. These results were subsequently extended to correlate LIN28A and LIN28B expression in multiple MB cell lines with cell viability, metabolism and stemness *in vitro*. For the first time, this study addressed the effects of LIN28A and LIN28B in MB, the results of which may lead to a new approach to target this devastating disease.

2 Materials And Methods

2.1 In-silico analysis of MB patient data

2.1.1 Platforms and datasets

LIN28A and LIN28B mRNA expression levels in multiple datasets were visualised, using R2 Genomics Analysis and Visualization Platform (http://r2.amc.nl) and GlioVis data portal (only used for patient survival analysis) [45]. The datasets used in this study include Harris [46], Sun [47], Donson [48], den Boer [49], Gilbertson [50], Pfister [51, 52], and Cavalli [6]. Datasets with either unclassified or not specified tissues were excluded to avoid bias interpretation and to keep data as consistent as possible among the datasets used (Table 1).

Table 1
Datasets used for *in-silico* analysis

Author	No. of Samples	No. of Normal Samples	No. of MB Samples	No. of other Tumours	Platform	Ref.
Harris	44	43	0	0	u133p2	[46]
Sun	180	23	0	153	u133p2	[47]
Donson	130	13	22	95	u133p2	[48]
den Boer	51	5	27	13	u133p2	[49]
Gilbertson	76	0	73	0	u133p2	[50]
Pfister	223	0	223	0	u133p2	[51, 52]
Cavalli	763	0	763	0	hugene11t	[6]

2.1.2 Expression analysis in brain tumours and normal brain tissue

The datasets by Harris [46], Sun [47], Donson [48], den Boer [49], Gilbertson [50] and Pfister [51, 52] were used to assess the expression of LIN28A and LIN28B genes in MB tissues compared to other brain tumours and normal brain tissues. Data were extracted from the R2 platform and plotted in GraphPad Prism Version 9.1 software for Windows (La Jolla, California, USA). Expression values are presented as log 2 values.

2.1.3 Expression in MB subgroups and normal brain samples

The datasets by Harris [46], Gilbertson [50] and Pfister [51, 52] were used to assess expression levels of LIN28A and LIN28B within four different MB subgroups and normal brain tissues. Data was extracted from the R2 platform and plotted in GraphPad Prism Version 9.1 software for Windows (La Jolla, California, USA). Expression values are presented as log 2 values.

2.1.4 Correlation of gene expression levels with tumour metastasis

The dataset by Cavalli [6] was used to conduct the expression of LIN28A and LIN28B genes in both metastatic and non-metastatic MB patients since it included the largest number of MB samples among the datasets used in this study as well as the metastatic status of patients at diagnosis (Table 1). Expression values were shown as log 2.

2.1.5 Stratification of MB patient survival rate by gene expression

Overall MB patient survival was analysed by Kaplan-Meier method using GlioVis portal and Cavalli cohort [6]. Median expression was used as a cut-off threshold to assign their high and low expression scores to MB patients for both LIN28A and LIN28B genes. Log-Rank test compared between high and the low expression groups. The hazard ratios (HR) with 95% confidence interval (CI), for LIN28A and LIN28B, are shown in Kaplan Meier plots. Data was extracted from GlioVis portal and plotted in GraphPad Prism.

2.2 Cell culture

Expression of LIN28A and LIN28B was assessed in five different MB cell lines (Daoy, D283, D341, CHLA-01-MED and CHLA-01R-MED) that belong to different MB molecular subgroups SHH (Daoy), G3 (D283 and D341) and G4 (CHLA-01-MED and CHLA-01R-MED). All cell lines were obtained from the American Type Culture Collection (ATCC; Manassas, Virginia, USA; Table 2). Daoy and D283 cells were cultured in Minimum Essential Medium Eagle (EMEM; #M0643; Sigma-Aldrich, St. Louis, MO, USA) supplemented with 10% foetal bovine serum (FBS), while D341 cells were supplemented with 20% FBS. CHLA-01-MED and CHLA-01R-MED were cultured in Dulbecco's Modified Eagle's Medium/Nutrient Mixture F-12 Ham (DMEM/F-12, 1:1 mixture; #D8900; Sigma-Aldrich) supplemented with 20 ng/ml EGF (Sigma-Aldrich), B-27™ Supplement (50x) (17504044; Gibco™; 2% final concentration (v/v); Sigma-Aldrich), and 20 ng/ml basic FGF (Sigma-Aldrich). Cells were maintained in a humidified incubator at 37°C and 5% CO_2. For this study, all cells used for experiments were cultured less than 10 passages.

Table 2
Description and characteristics of the five MB cell lines

Cell Lines	Organism	Tissue	Culture properties	Age, Gender and Ethnicity	Catalog Number
Daoy (corresponding to SHH molecular subgroup of MB)	Homo sapiens (Human)	Brain/ Cerebellum	Adherent	4 years Caucasian male	ATCC® HTB-186™
D283 (corresponding to Group 3/or 4 molecular subgroup of MB)	Homo sapiens (Human)	Brain/ Cerebellum; derived from metastatic site: peritoneum	Suspension and some adherent	6 years Caucasian male	ATCC® HTB-185™
D341 (corresponding to Group 3 molecular subgroup of MB)	Homo sapiens (Human)	Brain/ Cerebellum	Suspension	3.5 years male	ATCC® HTB-187™
CHLA-01-MED (corresponding to Group 4 molecular subgroup of MB)	Homo sapiens (Human)	Brain/ Brain Tumor	Suspension	8 years male	ATCC® CRL-3021™
CHLA-01R-MED (corresponding to Group 4 molecular subgroup of MB)	Homo sapiens (Human)	Brain; derived from Metastatic site: pleural fluid	Suspension	8 years male	ATCC® CRL-3034™

2.3 RNA extraction and quantitative real-time PCR

Six cell lysates of three biological replicates (each in duplicate) were prepared for each cell line for qPCR analysis. Isolation and purification of RNA was performed using ISOLATE II RNA Mini Kit (BIO-52073; Bioline, London, UK). Concentration and quality of total isolated RNA were measured using NanoDrop™ 1000 (ND-100) Spectrophotometer (Thermo Scientific, Waltham, Massachusetts, USA). RNA purity was quantified by A260/A280 nm and A260/A230 nm absorbance ratio. RNA samples were stored at − 80° C freezer until needed for complementary DNA (cDNA) synthesis. Total purified RNA was reverse transcribed to prepare cDNA using SensiFAST™ cDNA Synthesis Kit (BIO-65054; Bioline) and T100™ Thermal Cycler machine (catalog# 1861096; Bio-Rad, Hercules, California, USA) where the reverse transcription process occurs. The samples were incubated under the following protocol: annealing primers (25° C for 10 minutes), reverse transcriptase activation (42° C for 15 minutes) followed by reverse transcriptase deactivation (85° C for 5 minutes) and hold (4° C). cDNA samples were stored at − 20° C freezer until required for amplification using real time RT-PCR (qPCR). The prepared 5 ng cDNA was amplified using SensiFAST™ Probe No-ROX Kit (BIO-98020; Bioline) with the following primers: LIN28A forward (5'-CTGGTGGAGTATTCTGTATTG-3) and reverse (5'-ACCTGTCTCCTTTTGATCTG-3); LIN28B forward (5'-CTTGAGTCAATACGGGTAAC-3') and reverse (5'-CATCTATCTCCCTTTGGTTTTC-3'); RN18S1 forward (5'-ATCGGGGATTGCAATTATTC-3') and reverse (5'-CTCACTAAACCATCCAATCG-3'). Forward and reverse primers of the gene of interest were designed using Sigma-Aldrich KiCqStart™ Primers software (*https*://www.kicqstart-primers-sigmaaldrich.com/KiCqStartPrimers.php) (Sigma-Aldrich, St. Louis, MO, USA). 18S ribosomal RNA (rRNA) was used as a housekeeping gene for this analysis. For cycling and quantification of target genes, CFX Connect™ Real-Time PCR Detection System with Starter Package (catalog# 1855200; Bio-Rad) was used under the following conditions: 95° C for 2 minutes (DNA polymerase activation) followed by 40 cycles of 95° C for 5 seconds (DNA hydrogen bond denaturation), 58° C for 10 seconds (annealing primers) and 72° C for 20 seconds (DNA elongation). Quantification of the target gene expression was calculated using the comparative threshold cycle C_T (ΔΔ C_T) method by normalizing the C_T value of the target genes (LIN28A and LIN28B) against 18S rRNA served as internal control. The resulted C_T values were used to calculate Δ C_T for both the target genes and the housekeeping gene using this formula (C_T *of LIN28B* or *LIN28A* − C_T *of 18S* rRNA). Next, ΔΔ C_T values were calculated using this formula (Δ C_T *of the sample* - Δ C_T *of the average control group*). Thereafter, fold change values were calculated using this Eq. 2^- *(ΔΔ* C_T*)* to compare the expression levels of genes in different MB cell lines. The results were analyzed through multiple statistical comparison analysis; One-way analysis of variance (ANOVA) with Tukey's test, by GraphPad Prism Version 9.1 software (see Results section for further details).

2.4 Immunoblotting analysis

Total protein extracts from each of the five MB cell lines were prepared in triplicate for western blotting analysis. Protein concentrations were determined using Bio-Rad DC Protein Assay (catalog#500 − 0116; Bio-Rad). 5, 10 and 20 µg of total protein samples were resolved on 10% Bis-Glycine-polyacrylamide gel

and transferred onto Amersham™ Protran™ 0.2 µm nitrocellulose (NC) blotting membrane (catalog#10600001; GE Healthcare Life science, Chicago, Illinois, USA). Membranes were blocked in blocking solution (tris-buffered saline (TBS), 0.1% Tween-20, 5% (w/v) non-fat dry milk powder). Proteins were detected using primary antibodies against LIN28A (Rabbit polyclonal; catalog# SAB2702125; Sigma-Aldrich; 1:1000 dilution), LIN28B (Rabbit polyclonal; catalog# HPA061745; Sigma-Aldrich; 1:1000 dilution), Prom1 (CD133) (Mouse monoclonal; catalog# 2F8C5; Sigma-Aldrich; 1:1000 dilution), and β-actin (Mouse monoclonal; catalog# A5441; Sigma-Aldrich; 1:10,000 dilution) was used as loading control. Horseradish peroxidase-conjugated (HRP) secondary antibodies; goat anti-rabbit (catalog# 170–6515; Bio-Rad; 1:3000 dilution) and goat anti-mouse IgG (catalog# 170–6516; Bio-Rad; 1:3000 dilution) were used. All antibodies were prepared in blocking solution. The membrane was incubated with primary antibodies (anti-LIN28A /or anti-LIN28B /or anti-Pom1 "CD133") at 4° C overnight, while β-actin and secondary antibodies were used at room temperature for 1 hour. Amersham^{TM} ECL^{TM} Prime Western Blotting Detection Reagent (code# RPN2236; GE Healthcare Life science) was used for visualizing imunnoreactivity. Digital images were recorded using an Amersham™ Imager 600 (code# 29083461; GE Healthcare Life science) and Chemi-Smart 5000 imager (Vilber Lourmat, Eberhardzell, Germany). Band densities were quantified using Image Lab^{TM} software version 6.0.1 (Bio-Rad) and normalized to β-actin. Relative protein expression represents band intensity of LIN28A and LIN28B normalized to β-actin. PageRuler™ Plus Prestained Protein Ladder (catalog#26620; Thermo Scientific) was used to determine molecular weights (kDa) of protein bands. Results were analyzed through multiple statistical comparison analysis; one-way ANOVA with Tukey's test, by GraphPad Prism software, Version 9.1.

2.5 Immunofluorescence analysis

Subcellular localization of LIN28B was determined in five different MB cells using immunofluorescent detection. MB suspension cell lines were seeded at 5×10^3 (Daoy) or 10^4 (D283, D341, CHLA-01-MED, and CHLA-01R-MED) cells/well in black 96-well plates (655090, µClear®, Greiner, Germany) precoated with poly-L-lysine (P4832, Sigma-Aldrich) for 60 min (1:1 in PBS, 50 µL/well). After 24 hours, cells were fixed with 4% formaldehyde for 10 minutes before they were permeabilized (0.5% Triton®-X100 in phosphate-buffered saline (PBS)) for 10 minutes. Subsequently, cells were blocked with 10% normal goat serum (catalog# G9023; Sigma-Aldrich) in PBST (0.1% Tween-20 in PBS) for 1 hour and exposed to primary antibody against LIN28B (Rabbit polyclonal; catalog# HPA061745; Sigma-Aldrich; 1:1000 dilution) overnight at 4° C. Secondary antibody (A-11070; Alexa Fluor 488) was added to the cells for 1 hour at room temperature. Nuclear staining was performed using DAPI dye (1 µM) for 10 minutes at room temperature. Images were recorded by a high-content cell imaging system (IN Cell Analyzer 2200, GE Healthcare Life Sciences) at 20x magnification. Intensity of LIN28B-fluorescence for each cell was automatically quantified using IN Carta Image Analysis Software (GE Healthcare Life Sciences). The images used in the analysis were acquired from 4 different fields per one well of each cell line from three independent experiments. Overall, 554 cells for Daoy cell line, 631 cells for D283 cell line, 150 cells for D341 cell line, 318 cells for CHLA-01 cell line, and 393 cells for CHLA-01R cell line were analysed in this experiment.

2.6 Pharmacological inhibition of LIN28

For pharmacological inhibition studies, Lin28 1632 inhibitor (CAS No. 108825-65-6; Catalog No. 6068; Tocris Bioscience, Minneapolis, MN, USA) was used. Cells were seeded at 1.5×10^3 (Daoy) or 10^4 (D283, D341, CHLA-01-MED, and CHLA-01R-MED) cells/well in transparent 96-well plates. 24 h post plating, cells were treated with Lin28 1632 inhibitor at three different concentrations (10, 50 and 150 µM) for 72 h. DMSO was used as solvent control. Protein was isolated 72 h post-treatment for western blotting analysis. All experiments were performed independently three times.

2.6.1 ATP levels and protein content

To assess the effect of Lin28 1632 pharmacological inhibitor on MB cell metabolism and viability, measurement of cellular ATP levels and proteins were obtained via a luminescent ATP assay and protein assay, respectively. MB cells were seeded as described above (section 2.6.) in transparent 96-well plates. 24 hours post seeding, LIN28 inhibitor (1632 compound) was added for 72 h as described above.

For ATP measurements, 72 h post treatment, cells were transferred to Eppendorf tubes, washed twice with sterile PBS and 40 µl of ATP lysis buffer (4 mM EDTA/ 0.2% Triton X100) was added to each tube for 5 minutes at room temperature. Thereafter, 10 µl of cell lysate was mixed with 90 µl of ATP assay buffer (300 µM d-luciferin, 5 µg/mL luciferase, 625 µM EDTA, 75 µM DTT, 6.25 mM $MgCl_2$, 25 mM HEPES, 1 mg/mL BSA in PBS, pH 7.4) in white 96-well plates, followed by immediate luminescence measurement using a Tecan Spark® multimode microplate reader (Männedorf, Switzerland). Relative luminescence (RLU) was standardised to the untreated control and expressed as %RLU.

The Bio-Rad DC Protein Assay (colorimetric Assay) was used to quantify the protein content from the cell lysates according to the manufacturer's protocol. Absorbance was measured in a transparent 96-well plates at 750 nm using Tecan Spark® multimode microplate reader. The luminescence signal was standardized on protein content and expressed as %RLU/protein [mg/ml].

2.6.2 Sphere formation

CHLA-01R cells at 3×10^4 cells/well were plated into black 96-well plates (655090, µClear®, Greiner, Germany) in serum-free media. After 5 days, cellular spheres were stained with 5 µM Hoechst 33342, and visualised using fluorescence microscopy (IN Cell Analyzer 2200) at 4x magnification. Spheres larger than 100 µM in diameter were quantified using ImageJ 1.49q software (NIH, Bethesda, MD, USA, website: https://imagej.nih.gov/ij/).

2.7 Expression analysis in the developing brain

Microarray data of the cerebellum were obtained from BrainSpan Atlas of the Developing Human Brain (www.brainspan.org). A total of 31 cerebellum samples of individuals from 12 post-conceptual weeks to 40 years were used (donor ID for each sample is stated in the respective figure). Expression values of

LIN28A (Ensembl ID ENSG00000131914) and LIN28B (Ensembl ID ENSG00000187772) are presented in reads per kilobase of transcript (RPKM).

2.8 Statistical analysis

All statistical analysis was performed using GraphPad Prism (Version 9.1 for Windows, La Jolla, California, USA). For *in-silico* data, non-parametric statistical analysis was used including Kruskal-Wallis test and multiple comparison statistical hypothesis testing with Dunn's multiple comparisons test (to compare gene expression differences between MB subgroups and normal tissue), and two-tailed unpaired Mann-Whitney test for statistical comparisons (to compare between maximum two groups). For *in-vitro* data, parametric statistical analysis was performed using both one-way analysis of variance (ANOVA) through Tukey's test for multiple statistical comparison analysis (to compare between more than two cell lines), and two-tailed unpaired t-test for statistical comparisons (to compare between only two different groups). Specific statistical tests and significance for each experiment are mentioned in the figure legend. Data was reported as mean ± standard deviation (± SD), with p values of < 0.05 to be considered as statistically significant.

3 Results

3.1 Expression of LIN28A and LIN28B in brain tumours and MB molecular subgroups

Expression levels of LIN28A and LIN28B in normal brain and different brain tumours including glioblastoma, astrocytoma, oligodenroglioma, ependymoma and medulloblastoma were compared. LIN28A expression was comparable across the tested groups and was only significantly higher ($p < 0.0001$) in oligodenrogliomas compared to the non-tumour tissues (Fig. 1a). In contrast, among tumour tissues, LIN28B expression was significantly higher only in medulloblastoma tissues compared to tissues from normal brain tissue (Fig. 1b). MB is classified into four molecular subgroups of WNT, SHH, Group 3 and Group 4. These molecular subgroups influence the prognostic variability between MB patients [3]. Therefore, LIN28A and LIN28B expression in normal brain was compared to the different molecular MB subgroups. LIN28A was expressed homogeneously across the different MB groups with a significantly lower expression in the SHH subgroup compared to normal tissue (Fig. 1c). In contrast, LIN28B, was highly overexpressed ($p < 0.0001$) in MB subgroups 3 and 4 compared to subgroups 1 and 2 and normal brain tissue (Fig. 1d).

3.2 Expression of LIN28A and LIN28B in MB metastasis and overall MB patient survival

Since MB groups 3 and 4 are associated with higher metastasis and lower patient survival [5, 6], LIN28A and LIN28B expression was correlated with metastasis rates and patient survival. LIN28A expression was not correlated with MB metastasis rates (Fig. 2a), while LIN28B expression was significantly ($p < 0.0001$) associated with the occurrence of metastatic tumours (Fig. 2b). To evaluate the association between

LIN28A and LIN28B levels and MB prognosis, the overall survival of 612 MB patients in the Cavalli cohort [6] was assessed, using Kaplan-Meier analysis. While there was no significant association between LIN28A expression and patient survival (Fig. 2c), MB patients with high LIN28B levels showed a significantly reduced overall survival (Fig. 2d). Collectively, LIN28B appears to be overexpressed in aggressive MB subgroups and its expression was association with elevated rates of metastasis and reduced survival. This data highlights the potential importance of LIN28B in MB initiation and/or progression and prompts further mechanistic studies *in vitro*.

3.3 LIN28A and LIN28B mRNA and protein expression in MB cell lines

To translate the patient data to *in vitro* conditions, LIN28A and LIN28B expression in multiple cell lines, representing the different molecular MB subgroups, was assessed. Expression of LIN28A mRNA (Fig. 3a) and protein (Fig. 3b and c) were not significantly different between the tested MB cell lines. In contrast, LIN28B mRNA levels were higher in Group 3 (D341) cells compared to other cell lines (Fig. 3d) and protein levels were higher in Group 3 (D341) and Group 4 (CHLA-01) cells compared to the other cell lines (Fig. 3e and f). Based on the differential expression of LIN28B in MB cell lines, protein expression was also assessed using immunostaining. LIN28B levels showed higher expression levels in D341, CHLA-01 and D283 cells (Fig. 3g and h).

3.4 Effect of LIN28 inhibition on LIN28A and LIN28B expression, cell viability and metabolism

To assess the importance of RNA binding of LIN28, the pharmacological LIN28 inhibitor, Lin28 1632, was used. The effect of this inhibitor on the expression of LIN28A and LIN28B in five MB cell lines, as well as their viability was tested. Given the known role of LIN28 in energy production in other cell models [53–59], we also assessed the effect of this inhibitor on the intracellular ATP levels. In none of the cell lines, LIN28 inhibition affected the expression of LIN28A. However, it decreased the expression of LIN28B in Daoy cells at the highest tested concentration (Fig. 4a and b) and in D283 cells in a concentration dependent manner (Fig. 4d and e). In addition, as quantified by relative protein content levels, LIN28 inhibition reduced cell growth of Daoy and D283 cells at 50 and 100 μM (Fig. 4c and f), and of D341 cells at the highest tested concentration (Fig. 4i), while it had no effect on the growth of CHLA-01 and CHLA-01R cells (Fig. 4l and O). Collectively, these data showed that LIN28 inhibition suppressed viability and LIN28B expression in some MB cell lines. This effect was most pronounced in D283 cells where LIN28B levels and cell viability were reduced by the inhibitor in a concentration dependent manner. To delineate the mechanism of this reduced cell viability, cellular ATP levels were measured as LIN28 was reported to promote ATP production via glucose oxidation [54]. Treatment of D283 cells with the LIN28 inhibitor did not significantly alter relative intracellular ATP levels (Fig. 5a), suggesting that LIN28 does not affect ATP synthesis in these cells.

3.5 LIN28 inhibition suppresses stemness of D283 and CHLA-01R MB cells

LIN28 was reported to regulate the expression of CD133 [28, 60], a stemness marker that is also involved in cell proliferation [61]. Given the observed suppression of cell proliferation by LIN28 inhibition, the effect of the LIN28 inhibitor on CD133 expression in D283 cells was assessed. Treatment with Lin28 1632, concentration dependently, reduced the expression of LIN28B and reduced cell growth. LIN28 inhibition significantly reduced the expression of CD133 at 150 μM in D283 cells (Fig. 5b and c). Since CD133 is also regulating cellular stemness, we also assessed if LIN28 inhibition affected sphere formation of CHLA-01R cancer cells, which is associated with cellular stemness [62–65]. Treatment of CHLA-01R cells with the LIN28 inhibitor, Lin28 1632, significantly supressed the formation of cell spheres in a concentration dependent manner (Fig. 5d and e).

3.6 Expression of LIN28A and LIN28B in the developing brain

Our previous results pointed towards a potential role of LIN28 in cellular stemness. As cells age, they reduce their stemness features [66, 67]. Medulloblastoma is a primary malignant tumour of the cerebellum that is rarely seen in adults and predominantly occurs in children, when cells possess enhanced stemness characteristics. Therefore, LIN28A and LIN28B expression was measured in the cerebellum of the developing brain at different time points. Using the Atlas of the Developing Human Brain dataset that includes cerebellar expression profiles from individuals between 12 weeks to 40 years of age (www.brainspan.org), LIN28A expression remained steady (Fig. 6a). In contrast, cerebellar LIN28B showed higher levels in the newborn brain that gradually decreased to very low or non-detectable levels at 37 weeks of age, which remained at this level into adulthood (Fig. 6b).

4 Discussion

This study assessed the expression of LIN28A and LIN28B in MB patient samples and cell lines and observed the effect of LIN28 inhibition on MB cell growth, metabolism and stemness. Our data demonstrate a significant upregulation of LIN28B gene expression in MB tissues compared to normal brain tissues. This upregulation, which was only observed in MB and not in other brain tumours, was specific for aggressive MB subgroups 3 and 4. LIN28B expression levels correlated with MB patient survival and metastasis rates. LIN28A levels, on the other hand, were not upregulated in MB and did not show any association with MB subgroups, patient survival or metastasis rates. These data suggest the value of LIN28B as a potential diagnostic biomarker for MB and its molecular subgroups, as well as a prognostic indicator of survival time. Several studies have correlated LIN28A and/or B levels with patient prognosis in other cancers. High LIN28 expression were shown to be associated with tumour aggressiveness and poor patient prognosis in oesophagus cancer [20]. Similarly, LIN28A expression was shown to serve as a prognostic marker for gastric carcinoma [33] and hepatocellular carcinoma [21], while LIN28B expression was proposed to be a novel prognostic marker in gastric adenocarcinoma [68] and oral squamous cell carcinoma [69].

To test if targeting LIN28 has the potential to control MB cells growth, we also assessed the effect of pharmacological inhibition of LIN28 *in vitro.* LIN28 inhibition was most effective in D283 cells, where concentration dependently reduced LIN28B expression as well as MB cell growth and the expression of stemness marker CD133. Since LIN28 inhibition did not affect the levels of intracellular ATP in D283 cells, it is more likely that reduced CD133 expression, which was reported to be involved in cell proliferation [61], accounted for the reduced cell growth observed in this study. Our data also showed that LIN28 inhibition suppressed MB sphere formation of MB cells, another key phenotype of cancer cells with stemness features [62–65], further suggesting a role of LIN28 in MB stemness. A major problem in treating MB (as observed with many different cancer types) is the treatment resistance of cell populations that display characteristics of stem cells in the core of a tumour mass. These cell populations can survive the treatment and eventually result in recurrence of tumours in a more aggressive way [70]. It is therefore critical to target these cancer cell subpopulations. Identification of LIN28 as a regulator of MB stemness is a significant first step towards future studies that need to investigate how pharmacological targeting LIN28B could be used to affect MB cell stemness and therefore their sensitivity towards different treatment modalities. Our results support previous studies in breast cancer [22, 71] and lung cancer cells [72] that demonstrated a role of LIN28 proteins in cancer cell stemness. Future studies can assess if LIN28 inhibition can suppress the resistance of MB cells to chemotherapeutic agents and/or radiation therapy. In addition, stemness is a key property related to MB leptomeningeal dissemination, the metastatic spread of tumour cells through the cerebrospinal fluid to the brain and spinal cord [70]. Future studies can assess whether LIN28 inhibition affects the metastatic characteristics of MB cells, such as cell migration, invasion, and epithelial-to mesenchymal transition (EMT). EMT is a process that plays a key role in the progression, dissemination, and therapy resistance of epithelial tumours; however, recent evidence suggests that EMT also promotes malignancy of nonepithelial tumours [73].

The present study showed that LIN28B is highly expressed in the cerebellum during the first few months after birth and subsequently shows a clear decrease with age. This is an intriguing observation since MB was shown to arise from disruptions in cerebellar development [74] and the role of LIN28 proteins in the regulation of various stages of neuronal development [16, 75–77]. Indeed, LIN28B was reported to regulate neuronal differentiation by modulating the expression of Staufen1, a protein that initiates post-transcriptional regulation, including mRNA export, relocation, translation and decay [75]. In addition, LIN28B promotes neural crest cell migration and leads to transformation of the trunk region of the developing embryo [78]. Future studies are warranted to assess if the observed altered expression of LIN28B in the developing cerebellum contributes to MB initiation.

To understand the role of LIN28 in MB cells, this study used the only commercially available pharmacological inhibitor of this protein to date, Lin28 1632 [79]. To better understand the isoform-specific roles of LIN28 proteins, siRNA-mediated silencing and/or plasmid over-expression studies, specifically targeting LIN28A and LIN28B genes, are needed in future studies. In addition, it is important to note that Lin28 1632, only inhibits the LIN28/let-7 interaction, while LIN28 proteins are known to regulate key biological functions via let-7 dependent and independent mechanisms [80]. Therefore, mechanistic studies are needed to delineate whether the observed LIN28 activities in MB cells observed in

this study, occur via let-7 dependent or let-7 independent pathways. However, at present there are no pharmacological inhibitors available commercially to inhibit the let-7 independent activities of LIN28. Therefore, the development of such compounds in the future will be invaluable to selectively modulate these two distinct signalling activities of LIN28.

Overall, the present study demonstrates the potential value of LIN28B as a diagnostic and prognostic marker for MB. It also, for the first time highlights the potential to use small molecule pharmacological antagonist of LIN28 to suppress MB cell growth and stemness, which could lead to a new therapeutic approach for the treatment of MB. Consequently, future studies need to test LIN28 inhibition in preclinical models of MB to explore the therapeutic potential of this approach as a future treatment strategy against MB.

Declarations

Ethical Approval and Consent to participate

Not applicable.

Consent for publication

Not applicable.

Availability of supporting data

Not applicable.

Competing interests

Authors declare no competing interest.

Funding

This research was funded by the Brain Foundation, Kids Cancer Project and Research Enhancement Program of the College of Health and Medicine, University of Tasmania.

Authors' contributions

Conceptualization: A.M., J.A.H., N.G., I.A.; Methodology: A.M., M.S., R.W.; Formal analysis and investigation: A.H., M.S., R.W.; Writing - original draft preparation: A.M., N.., I.A.; Writing - review and editing: A.M., M.S., R.W., J.A.H., N.G., I.A.; Funding acquisition: J.A.H., N.G., I.A.; Supervision: N.G., I.A.

Acknowledgements

Not applicable.

References

1. W.R. Polkinghorn, N.J. Tarbell, Medulloblastoma: tumorigenesis, current clinical paradigm, and efforts to improve risk stratification. Nat. Reviews Clin. Oncol. **4**, 295 (2007)
2. J. Hildebrand, D. Balériaux. I.V. Part, *Sporadic Diseases; 17 Cerebellar disorders in cancer. The Cerebellum and Its Disorders* (Cambridge University Press, 2002), pp. 265–287
3. V. Ramaswamy, M. Remke, E. Bouffet, S. Bailey, S.C. Clifford, F. Doz, M. Kool, C. Dufour, G. Vassal, T. Milde, O. Witt, K. von Hoff, T. Pietsch, P.A. Northcott, A. Gajjar, G.W. Robinson, L. Padovani, N. André, M. Massimino, B. Pizer, R. Packer, S. Rutkowski, S.M. Pfister, M.D. Taylor, S.L. Pomeroy, Risk stratification of childhood medulloblastoma in the molecular era: the current consensus. Acta Neuropathol. **131**, 821–831 (2016). doi:10.1007/s00401-016-1569-6
4. D.W. Ellison, Childhood medulloblastoma: novel approaches to the classification of a heterogeneous disease. Acta Neuropathol. **120**, 305–316 (2010). doi:10.1007/s00401-010-0726-6
5. M.D. Taylor, P.A. Northcott, A. Korshunov, M. Remke, Y.-J. Cho, S.C. Clifford, C.G. Eberhart, D.W. Parsons, S. Rutkowski, A. Gajjar, D.W. Ellison, P. Lichter, R.J. Gilbertson, S.L. Pomeroy, M. Kool, S.M. Pfister, Molecular subgroups of medulloblastoma: the current consensus. Acta Neuropathol. **123**, 465–472 (2012). doi:10.1007/s00401-011-0922-z
6. F.M.G. Cavalli, M. Remke, L. Rampasek, J. Peacock, D.J.H. Shih, M.D. Taylor, Intertumoral Heterogeneity within Medulloblastoma Subgroups. Cancer Cell. **31**, 737–754.e736 (2017). doi:10.1016/j.ccell.2017.05.005
7. J.R. Crawford, T.J. MacDonald, R.J. Packer, Medulloblastoma in childhood: new biological advances. Lancet Neurol. **6**, 1073–1085 (2007). doi:https://doi.org/10.1016/S1474-4422(07)70289-2
8. A.M. Maddrey, J.A. Bergeron, E.R. Lombardo, N.K. McDonald, A.F. Mulne, P.D. Barenberg, D.C. Bowers, Neuropsychological performance and quality of life of 10 year survivors of childhood medulloblastoma. J. Neurooncol. **72**, 245–253 (2005). doi:10.1007/s11060-004-3009-z
9. E.G. Moss, L. Tang, Conservation of the heterochronic regulator Lin-28, its developmental expression and microRNA complementary sites. Dev. Biol. **258**, 432–442 (2003). doi:10.1016/s0012-1606(03)00126-x
10. Y. Guo, Y. Chen, H. Ito, A. Watanabe, X. Ge, T. Kodama, H. Aburatani, Identification and characterization of lin-28 homolog B (LIN28B) in human hepatocellular carcinoma. Gene **384**, 51–61 (2006). doi:https://doi.org/10.1016/j.gene.2006.07.011
11. V. Ambros, H. Horvitz, Heterochronic mutants of the nematode Caenorhabditis elegans. Science **226**, 409–416 (1984). doi:10.1126/science.6494891
12. E.G. Moss, R.C. Lee, V. Ambros, The Cold Shock Domain Protein LIN-28 Controls Developmental Timing in C. elegans and Is Regulated by the lin-4 RNA, 88, 637–646 (1997) doi: 10.1016/s0092-8674(00)81906-6
13. A. Polesskaya, S. Cuvellier, I. Naguibneva, A. Duquet, E.G. Moss, A. Harel-Bellan, Lin-28 binds IGF-2 mRNA and participates in skeletal myogenesis by increasing translation efficiency, 21, 1125–1138

(2007) doi: 10.1101/gad.415007

14. J.A. West, S.R. Viswanathan, A. Yabuuchi, K. Cunniff, A. Takeuchi, I.H. Park, J.E. Sero, H. Zhu, A. Perez-Atayde, A.L. Frazier, M.A. Surani, G.Q. Daley, A role for Lin28 in primordial germ-cell development and germ-cell malignancy. Nature **460**, 909–913 (2009). doi:10.1038/nature08210
15. E. Balzer, C. Heine, Q. Jiang, V.M. Lee, E.G. Moss, LIN28 alters cell fate succession and acts independently of the let-7 microRNA during neurogliogenesis in vitro. Development **137**, 891–900 (2010). doi:10.1242/dev.042895
16. M. Yang, S.L. Yang, S. Herrlinger, C. Liang, M. Dzieciatkowska, K.C. Hansen, R. Desai, A. Nagy, L. Niswander, E.G. Moss, J.F. Chen, Lin28 promotes the proliferative capacity of neural progenitor cells in brain development. Development **142**, 1616–1627 (2015). doi:10.1242/dev.120543
17. J.F. de Vasconcellos, R.M. Fasano, Y.T. Lee, M. Kaushal, C. Byrnes, E.R. Meier, M. Anderson, A. Rabel, R. Braylan, D.F. Stroncek, J.L. Miller, LIN28A Expression Reduces Sickling of Cultured Human Erythrocytes. PLOS ONE **9**, e106924 (2014). doi:10.1371/journal.pone.0106924
18. H. Ma, S. Yu, X. Liu, Y. Zhang, T. Fakadej, Z. Liu, C. Yin, W. Shen, J.W. Locasale, J.M. Taylor, L. Qian, J. Liu, Lin28a Regulates Pathological Cardiac Hypertrophic Growth Through Pck2-Mediated Enhancement of Anabolic Synthesis. Circulation **139**, 1725–1740 (2019). doi:10.1161/CIRCULATIONAHA.118.037803 doi
19. H. Zhu, N. Shyh-Chang, G. Ayellet, A. Shinoda, Samar, William, J. Takeuchi, Jesse, A. Michael, R. Urbach, James, D. Triboulet, Richard, Altshuler and George, The Lin28/let-7 Axis Regulates Glucose Metabolism. Cell **147**, 81–94 (2011). doi:10.1016/j.cell.2011.08.033
20. R. Hamano, H. Miyata, M. Yamasaki, K. Sugimura, K. Tanaka, Y. Kurokawa, K. Nakajima, S. Takiguchi, Y. Fujiwara, M. Mori, Y. Doki, High expression of Lin28 is associated with tumour aggressiveness and poor prognosis of patients in oesophagus cancer, 106, 1415–1423 (2012) doi: 10.1038/bjc.2012.90
21. J.-L. Qiu, P.-Z. Huang, J.-H. You, R.-H. Zou, L. Wang, J. Hong, B.-K. Li, K. Zhou, Y.-F. Yuan, LIN28 expression and prognostic value in hepatocellular carcinoma patients who meet the Milan criteria and undergo hepatectomy. Chin. J. Cancer **31**, 223–232 (2012). doi:10.5732/cjc.011.10426
22. Y. Liu, H. Li, J. Feng, X. Cui, W. Huang, Y. Li, F. Su, Q. Liu, J. Zhu, X. Lv, J. Chen, D. Huang, F. Yu, Lin28 Induces Epithelial-to-Mesenchymal Transition and Stemness via Downregulation of Let-7a in Breast Cancer Cells, 8, e83083 (2013) doi: 10.1371/journal.pone.0083083
23. C. Feng, V. Neumeister, W. Ma, J. Xu, L. Lu, J. Bordeaux, N.J. Maihle, D.L. Rimm, Y. Huang, Lin28 regulates HER2 and promotes malignancy through multiple mechanisms. Cell. Cycle **11**, 2486–2494 (2012). doi:10.4161/cc.20893
24. D. Xue, Y. Peng, F. Wang, R.W. Allan, D. Cao, RNA-binding protein LIN28 is a sensitive marker of ovarian primitive germ cell tumours, 59, 452–459 (2011) doi: 10.1111/j.1365-2559.2011.03949.x
25. D. Cao, A. Liu, F. Wang, R.W. Allan, K. Mei, Y. Peng, J. Du, S. Guo, T.W. Abel, Z. Lane, J. Ma, M. Rodriguez, S. Akhi, N. Dehiya, J. Li, RNA-binding protein LIN28 is a marker for primary extragonadal germ cell tumors: an immunohistochemical study of 131 cases. Mod. Pathol. **24**, 288–296 (2011). doi:10.1038/modpathol.2010.195

26. D. Cao, R.W. Allan, L. Cheng, Y. Peng, C.C. Guo, N. Dahiya, S. Akhi, J. Li, RNA-binding protein LIN28 is a marker for testicular germ cell tumors, 42, 710–718 (2011) doi: 10.1016/j.humpath.2010.09.007
27. C.E. King, L. Wang, R. Winograd, B.B. Madison, P.S. Mongroo, C.N. Johnstone, A.K. Rustgi, LIN28B fosters colon cancer migration, invasion and transformation through let-7-dependent and -independent mechanisms, 30, 4185–4193 (2011) doi: 10.1038/onc.2011.131
28. C.E. King, M. Cuatrecasas, A. Castells, A.R. Sepulveda, J.S. Lee, A.K. Rustgi, LIN28B Promotes Colon Cancer Progression and Metastasis. Cancer Res. **71**, 4260–4268 (2011). doi:10.1158/0008-5472.can-10-4637
29. K.F. Hsu, M.R. Shen, Y.F. Huang, Y.M. Cheng, S.H. Lin, N.H. Chow, S.W. Cheng, C.Y. Chou, C.L. Ho, Overexpression of the RNA-binding proteins Lin28B and IGF2BP3 (IMP3) is associated with chemoresistance and poor disease outcome in ovarian cancer. Br. J. Cancer **113**, 414–424 (2015). doi:10.1038/bjc.2015.254
30. L. Lu, D. Katsaros, S.T. Mayne, H.A. Risch, C. Benedetto, E.M. Canuto, H. Yu, Functional study of risk loci of stem cell-associated gene lin-28B and associations with disease survival outcomes in epithelial ovarian cancer. Carcinogenesis **33**, 2119–2125 (2012). doi:10.1093/carcin/bgs243
31. L. Lu, D. Katsaros, K. Shaverdashvili, B. Qian, Y. Wu, I.A.R. de la Longrais, M. Preti, G. Menato, H. Yu, Pluripotent factor lin-28 and its homologue lin-28b in epithelial ovarian cancer and their associations with disease outcomes and expression of let-7a and IGF-II. Eur. J. Cancer **45**, 2212–2218 (2009)
32. Q. Wang, J. Zhou, J. Guo, R. Teng, J. Shen, Y. Huang, S. Xie, Q. Wei, W. Zhao, W. Chen, X. Yuan, Y. Chen, L. Wang, Lin28 promotes Her2 expression and Lin28/Her2 predicts poorer survival in gastric cancer. Tumor Biology **35**, 11513–11521 (2014). doi:10.1007/s13277-014-2481-0
33. C. Xu, J. Shen, S. Xie, Z. Jiang, L. Huang, L. Wang, Positive expression of Lin28 is correlated with poor survival in gastric carcinoma, 30, (2013) doi: 10.1007/s12032-012-0382-x
34. S.R. Viswanathan, J.T. Powers, W. Einhorn, Y. Hoshida, T.L. Ng, S. Toffanin, M. O'Sullivan, J. Lu, L.A. Phillips, V.L. Lockhart, S.P. Shah, P.S. Tanwar, C.H. Mermel, R. Beroukhim, M. Azam, J. Teixeira, M. Meyerson, T.P. Hughes, J.M. Llovet, J. Radich, C.G. Mullighan, T.R. Golub, P.H. Sorensen, G.Q. Daley, Lin28 promotes transformation and is associated with advanced human malignancies. Nat. Genet. **41**, 843–848 (2009). doi:10.1038/ng.392
35. J. Zhou, Z.-L. Chan, C. Bi, X. Lu, P.S. Chong, J.-Y. Chooi, L.L. Cheong, S.-C. Liu, Y.Q. Ching, Y. Zhou, M. Osato, T.Z. Tan, C.H. Ng, S.-B. Ng, Q. Zeng, W.J. Chng, LIN28B Activation by PRL-3 Promotes Leukemogenesis and a Stem Cell-like Transcriptional Program in AML, molcanres.0275.0272 (2016) doi: 10.1158/1541-7786.mcr-16-0275-t
36. A. Urbach, A. Yermalovich, J. Zhang, C.S. Spina, H. Zhu, A.R. Perez-Atayde, R. Shukrun, J. Charlton, N. Sebire, W. Mifsud, B. Dekel, K. Pritchard-Jones, G.Q. Daley, Lin28 sustains early renal progenitors and induces Wilms tumor. Genes Dev. **28**, 971–982 (2014). doi:10.1101/gad.237149.113
37. S.J. Diskin, M. Capasso, R.W. Schnepp, K.A. Cole, E.F. Attiyeh, C. Hou, M. Diamond, E.L. Carpenter, C. Winter, H. Lee, J. Jagannathan, V. Latorre, A. Iolascon, H. Hakonarson, M. Devoto, J.M. Maris,

Common variation at 6q16 within HACE1 and LIN28B influences susceptibility to neuroblastoma. Nat. Genet. **44**, 1126–1130 (2012). doi:10.1038/ng.2387

38. R. Qin, J. Zhou, C. Chen, T. Xu, Y. Yan, Y. Ma, Z. Zheng, Y. Shen, Y. Lu, D. Fu, J. Chen, LIN28 Is Involved in Glioma Carcinogenesis and Predicts Outcomes of Glioblastoma Multiforme Patients, 9, e86446 (2014) doi: 10.1371/journal.pone.0086446
39. X.-G. Mao, M. Hütt-Cabezas, B.A. Orr, M. Weingart, I. Taylor, A.K.D. Rajan, Y. Odia, U. Kahlert, J. Maciaczyk, G. Nikkhah, C.G. Eberhart, E.H. Raabe, LIN28A facilitates the transformation of human neural stem cells and promotes glioblastoma tumorigenesis through a pro-invasive genetic program. Oncotarget **4**, 1050–1064 (2013). doi:10.18632/oncotarget.1131
40. J. Lu, X. Liu, J. Zheng, J. Song, Y. Liu, X. Ruan, S. Shen, L. Shao, C. Yang, D. Wang, H. Cai, S. Cao, Y. Xue, Lin28A promotes IRF6-regulated aerobic glycolysis in glioma cells by stabilizing SNHG14, Cell Death Dis. 11, (2020) doi:10.1038/s41419-020-2650-6
41. A. Korshunov, M. Ryzhova, D.T.W. Jones, P.A. Northcott, P. Van Sluis, R. Volckmann, J. Koster, R. Versteeg, C. Cowdrey, A. Perry, D. Picard, M. Rosenblum, F. Giangaspero, E. Aronica, U. Schüller, M. Hasselblatt, V.P. Collins, A. Von Deimling, P. Lichter, A. Huang, S.M. Pfister, M. Kool, LIN28A immunoreactivity is a potent diagnostic marker of embryonal tumor with multilayered rosettes (ETMR). Acta Neuropathol. **124**, 875–881 (2012). doi:10.1007/s00401-012-1068-3
42. P. Sin-Chan, I. Mumal, T. Suwal, B. Ho, X. Fan, I. Singh, Y. Du, M. Lu, N. Patel, J. Torchia, D. Popovski, M. Fouladi, P. Guilhamon, J.R. Hansford, S. Leary, L.M. Hoffman, J.M. Mulcahy Levy, A. Lassaletta, P. Solano-Paez, E. Rivas, A. Reddy, G.Y. Gillespie, N. Gupta, T.E. Van Meter, H. Nakamura, T.-T. Wong, Y.-S. Ra, S.-K. Kim, L. Massimi, R.G. Grundy, J. Fangusaro, D. Johnston, J. Chan, L. Lafay-Cousin, E.I. Hwang, Y. Wang, D. Catchpoole, J. Michaud, B. Ellezam, R. Ramanujachar, H. Lindsay, M.D. Taylor, C.E. Hawkins, E. Bouffet, N. Jabado, S.K. Singh, C.L. Kleinman, D. Barsyte-Lovejoy, X.-N. Li, P.B. Dirks, C.Y. Lin, S.C. Mack, J.N. Rich, A. Huang, A C19MC-LIN28A-MYCN Oncogenic Circuit Driven by Hijacked Super-enhancers Is a Distinct Therapeutic Vulnerability in ETMRs: A Lethal Brain Tumor. Cancer Cell. **36**, 51–67.e57 (2019). doi:10.1016/j.ccell.2019.06.002
43. S.A. Choi, S.-K. Kim, J.Y. Lee, K.-C. Wang, C. Lee, J.H. Phi, LIN28B is highly expressed in atypical teratoid/rhabdoid tumor (AT/RT) and suppressed through the restoration of SMARCB1, 16, (2016) doi: 10.1186/s12935-016-0307-4
44. M.F. Weingart, J.J. Roth, M. Hutt-Cabezas, T.M. Busse, H. Kaur, A. Price, R. Maynard, J. Rubens, I. Taylor, X.-G. Mao, J. Xu, Y. Kuwahara, S.J. Allen, A. Erdreich-Epstein, B.E. Weissman, B.A. Orr, C.G. Eberhart, J.A. Biegel, E.H. Raabe, Disrupting LIN28 in atypical teratoid rhabdoid tumors reveals the importance of the mitogen activated protein kinase pathway as a therapeutic target. Oncotarget **6**, 3165–3177 (2015). doi:10.18632/oncotarget.3078
45. R.L. Bowman, Q. Wang, A. Carro, R.G.W. Verhaak, M. Squatrito, GlioVis data portal for visualization and analysis of brain tumor expression datasets, Neuro Oncol. 19, 139–141 (2017) doi:10.1093/neuonc/now247

46. L.W. Harris, H.E. Lockstone, P. Khaitovich, C.S. Weickert, M.J. Webster, S. Bahn, Gene expression in the prefrontal cortex during adolescence: implications for the onset of schizophrenia. BMC Med. Genomics **2**, 28 (2009). doi:10.1186/1755-8794-2-28

47. L. Sun, A.M. Hui, Q. Su, A. Vortmeyer, Y. Kotliarov, S. Pastorino, A. Passaniti, J. Menon, J. Walling, R. Bailey, M. Rosenblum, T. Mikkelsen, H.A. Fine, Neuronal and glioma-derived stem cell factor induces angiogenesis within the brain. Cancer Cell. **9**, 287–300 (2006). doi:10.1016/j.ccr.2006.03.003

48. A.M. Griesinger, D.K. Birks, A.M. Donson, V. Amani, L.M. Hoffman, A. Waziri, M. Wang, M.H. Handler, N.K. Foreman, Characterization of distinct immunophenotypes across pediatric brain tumor types, Journal of immunology (Baltimore, Md.: 1950) 191, 4880–4888 (2013) doi: 10.4049/jimmunol.1301966

49. J.M. de Bont, J.M. Kros, M.M. Passier, R.E. Reddingius, P.A. Sillevis Smitt, T.M. Luider, M.L. den Boer, R. Pieters, Differential expression and prognostic significance of SOX genes in pediatric medulloblastoma and ependymoma identified by microarray analysis. Neuro Oncol. **10**, 648–660 (2008). doi:10.1215/15228517-2008-032

50. G. Robinson, M. Parker, T.A. Kranenburg, C. Lu, X. Chen, L. Ding, T.N. Phoenix, E. Hedlund, L. Wei, X. Zhu, N. Chalhoub, S.J. Baker, R. Huether, R. Kriwacki, N. Curley, R. Thiruvenkatam, J. Wang, G. Wu, M. Rusch, X. Hong, J. Becksfort, P. Gupta, J. Ma, J. Easton, B. Vadodaria, A. Onar-Thomas, T. Lin, S. Li, S. Pounds, S. Paugh, D. Zhao, D. Kawauchi, M.F. Roussel, D. Finkelstein, D.W. Ellison, C.C. Lau, E. Bouffet, T. Hassall, S. Gururangan, R. Cohn, R.S. Fulton, L.L. Fulton, D.J. Dooling, K. Ochoa, A. Gajjar, E.R. Mardis, R.K. Wilson, J.R. Downing, J. Zhang, R.J. Gilbertson, Novel mutations target distinct subgroups of medulloblastoma. Nature **488**, 43–48 (2012). doi:10.1038/nature11213

51. R2: Genomics Analysis and Visualization Platform http://r2.amc.nl Accessed 19 December 2019

52. P.A. Northcott, I. Buchhalter, A.S. Morrissy, V. Hovestadt, J. Weischenfeldt, T. Ehrenberger, S. Gröbner, M. Segura-Wang, T. Zichner, V.A. Rudneva, H.-J. Warnatz, N. Sidiropoulos, A.H. Phillips, S. Schumacher, K. Kleinheinz, S.M. Waszak, S. Erkek, D.T.W. Jones, B.C. Worst, M. Kool, M. Zapatka, N. Jäger, L. Chavez, B. Hutter, M. Bieg, N. Paramasivam, M. Heinold, Z. Gu, N. Ishaque, C. Jäger-Schmidt, C.D. Imbusch, A. Jugold, D. Hübschmann, T. Risch, V. Amstislavskiy, F.G.R. Gonzalez, U.D. Weber, S. Wolf, G.W. Robinson, X. Zhou, G. Wu, D. Finkelstein, Y. Liu, F.M.G. Cavalli, B. Luu, V. Ramaswamy, X. Wu, J. Koster, M. Ryzhova, Y.-J. Cho, S.L. Pomeroy, C. Herold-Mende, M. Schuhmann, M. Ebinger, L.M. Liau, J. Mora, R.E. McLendon, N. Jabado, T. Kumabe, E. Chuah, Y. Ma, R.A. Moore, A.J. Mungall, K.L. Mungall, N. Thiessen, K. Tse, T. Wong, S.J.M. Jones, O. Witt, T. Milde, A. Von Deimling, D. Capper, A. Korshunov, M.-L. Yaspo, R. Kriwacki, A. Gajjar, J. Zhang, R. Beroukhim, E. Fraenkel, J.O. Korbel, B. Brors, M. Schlesner, R. Eils, M.A. Marra, S.M. Pfister, Nature **547**, 311–317 (2017). doi:10.1038/nature22973 M.D. Taylor and P. Lichter, The whole-genome landscape of medulloblastoma subtypes

53. N. Shyh-Chang, George, Lin28: Primal Regulator of Growth and Metabolism in Stem Cells. Cell. Stem Cell. **12**, 395–406 (2013). doi:10.1016/j.stem.2013.03.005

54. N. Shyh-Chang, H. Zhu, T.G. Shinoda, L. Marc, Kaloyan, Nguyen, John, Lewis and George, Lin28 Enhances Tissue Repair by Reprogramming Cellular Metabolism. Cell **155**, 778–792 (2013).

doi:10.1016/j.cell.2013.09.059

55. M.D. Burkhalter, Y. Morita, K.L. Rudolph, Lin28a–boost your energy for youthful regeneration. EMBO J. **33**, 5–6 (2014). doi:10.1002/embj.201387363
56. C.K. Docherty, I.P. Salt, J.R. Mercer, Lin28A induces energetic switching to glycolytic metabolism in human embryonic kidney cells. Stem Cell Res. Ther. **7**, 78 (2016). doi:10.1186/s13287-016-0323-2
57. X. Ma, C. Li, L. Sun, D. Huang, T. Li, X. He, G. Wu, Z. Yang, X. Zhong, L. Song, P. Gao, H. Zhang, Lin28/let-7 axis regulates aerobic glycolysis and cancer progression via PDK1. Nat. Commun. **5**, 5212 (2014). doi:10.1038/ncomms6212
58. H. Zhu, N. Shyh-Chang, A.V. Segrè, G. Shinoda, S.P. Shah, W.S. Einhorn, A. Takeuchi, J.M. Engreitz, J.P. Hagan, M.G. Kharas, A. Urbach, J.E. Thornton, R. Triboulet, R.I. Gregory, D. Consortium, M. Investigators, D. Altshuler, G.Q. Daley, The Lin28/let-7 axis regulates glucose metabolism. Cell **147**, 81–94 (2011). doi:10.1016/j.cell.2011.08.033
59. M. Zhang, X. Niu, J. Hu, Y. Yuan, S. Sun, J. Wang, W. Yu, C. Wang, D. Sun, H. Wang, Lin28a Protects against Hypoxia/Reoxygenation Induced Cardiomyocytes Apoptosis by Alleviating Mitochondrial Dysfunction under High Glucose/High Fat Conditions. PLOS ONE **9**, e110580 (2014). doi:10.1371/journal.pone.0110580
60. Y. Zhong, L. Cao, H. Ma, Q. Wang, P. Wei, J. Yang, Y. Mo, L. Cao, C. Shuai, S. Peng, Lin28A Regulates Stem-like Properties of Ovarian Cancer Cells by Enriching RAN and HSBP1 mRNA and Up-regulating its Protein Expression. Int. J. Biol. Sci. **16**, 1941–1953 (2020). doi:10.7150/ijbs.43504
61. H. Tang, Y. Gong, Y. Mao, Q. Xie, M. Zheng, D. Wang, H. Zhu, X. Wang, H. Chen, X. Chen, L. Zhou, CD133-positive cells might be responsible for efficient proliferation of human meningioma cells. Int. J. Mol. Sci. **13**, 6424–6439 (2012). doi:10.3390/ijms13056424
62. E. Pastrana, V. Silva-Vargas, F. Doetsch, Eyes Wide Open: A Critical Review of Sphere-Formation as an Assay for Stem Cells. Cell. Stem Cell. **8**, 486–498 (2011). doi:https://doi.org/10.1016/j.stem.2011.04.007
63. J.S. Yakisich, N. Azad, R. Venkatadri, Y. Kulkarni, C. Wright, V. Kaushik, A.K.V. Iyer, Formation of Tumorspheres with Increased Stemness without External Mitogens in a Lung Cancer Model, Stem Cells Int 2016, 5603135–5603135 (2016) doi: 10.1155/2016/5603135
64. L. Cao, Y. Zhou, B. Zhai, J. Liao, W. Xu, R. Zhang, J. Li, Y. Zhang, L. Chen, H. Qian, M. Wu, Z. Yin, Sphere-forming cell subpopulations with cancer stem cell properties in human hepatoma cell lines. BMC Gastroenterol. **11**, 71 (2011). doi:10.1186/1471-230X-11-71
65. J. Xu, A.S. Margol, A. Shukla, X. Ren, J.L. Finlay, M.D. Krieger, F.H. Gilles, F.J. Couch, M. Aziz, E.T. Fung, S. Asgharzadeh, M.T. Barrett, and A. Erdreich-Epstein, Disseminated Medulloblastoma in a Child with Germline BRCA2 6174delT Mutation and without Fanconi Anemia. Front. Oncol. **5**, 191–191 (2015). doi:10.3389/fonc.2015.00191
66. B. Bose, S.S. P, Aging induced loss of stemness with concomitant gain of myogenic properties of a pure population of CD34+/CD45 – muscle derived stem cells. Int. J. Biochem. Cell Biol. **70**, 1–12 (2016). doi:https://doi.org/10.1016/j.biocel.2015.10.009

67. A.S.I. Ahmed, M.H. Sheng, S. Wasnik, D.J. Baylink, K.-H.W. Lau, Effect of aging on stem cells. World J. Exp. Med. **7**, 1–10 (2017). doi:10.5493/wjem.v7.i1.1

68. Q. Hu, J. Peng, W. Liu, X. He, L. Cui, X. Chen, M. Yang, H. Liu, S. Liu, H. Wang, Lin28B is a novel prognostic marker in gastric adenocarcinoma. Int. J. Clin. Exp. Pathol. **7**, 5083–5092 (2014)

69. T. Wu, J. Jia, X. Xiong, H. He, L. Bu, Z. Zhao, C. Huang, W. Zhang, Increased Expression of Lin28B Associates with Poor Prognosis in Patients with Oral Squamous Cell Carcinoma. PLoS ONE **8**, e83869 (2013). doi:10.1371/journal.pone.0083869

70. G.H. Huang, Q.F. Xu, Y.H. Cui, N. Li, X.W. Bian, S.Q. Lv, Medulloblastoma stem cells: Promising targets in medulloblastoma therapy. Cancer Sci. **107**, 583–589 (2016). doi:10.1111/cas.12925

71. C. Chen, L. Bai, F. Cao, S. Wang, H. He, M. Song, H. Chen, Y. Liu, J. Guo, Q. Si, Y. Pan, R. Zhu, T.-H. Chuang, R. Xiang, Y. Luo, Targeting LIN28B reprograms tumor glucose metabolism and acidic microenvironment to suppress cancer stemness and metastasis. Oncogene **38**, 4527–4539 (2019). doi:10.1038/s41388-019-0735-4

72. R. Zhang, P. Liu, X. Zhang, Y. Ye, J. Yu, Lin28A promotes the proliferation and stemness of lung cancer cells via the activation of mitogen-activated protein kinase pathway dependent on microRNA let-7c. Annals of Translational Medicine **9**, 982 (2021)

73. U.D. Kahlert, J.V. Joseph, F.A.E. Kruyt, EMT- and MET-related processes in nonepithelial tumors: importance for disease progression, prognosis, and therapeutic opportunities. Mol. Oncol. **11**, 860–877 (2017). doi:https://doi.org/10.1002/1878-0261.12085

74. S. Marino, Medulloblastoma: developmental mechanisms out of control. Trends Mol. Med. **11**, 17–22 (2005). doi:10.1016/j.molmed.2004.11.008

75. Y. Oh, J. Park, J.-I. Kim, M.-Y. Chang, S.-H. Lee, Y.-H. Cho, J. Hwang, Lin28B and miR-142-3p regulate neuronal differentiation by modulating Staufen1 expression. Cell. Death & Differentiation **25**, 432–443 (2018). doi:10.1038/cdd.2017.182

76. J.S. Nowak, N.R. Choudhury, F. de Lima Alves, J. Rappsilber, G. Michlewski, Lin28a regulates neuronal differentiation and controls miR-9 production. Nat. Commun. **5**, 3687 (2014). doi:10.1038/ncomms4687

77. J.S. Romer-Seibert, N.W. Hartman, E.G. Moss, The RNA-binding protein LIN28 controls progenitor and neuronal cell fate during postnatal neurogenesis. FASEB J. **33**, 3291–3303 (2019). doi:https://doi.org/10.1096/fj.201801118R

78. D. Corallo, M. Donadon, M. Pantile, V. Sidarovich, S. Cocchi, M. Ori, M. De Sarlo, S. Candiani, C. Frasson, M. Distel, A. Quattrone, C. Zanon, G. Basso, G.P. Tonini, S. Aveic, LIN28B increases neural crest cell migration and leads to transformation of trunk sympathoadrenal precursors. Cell. Death & Differentiation **27**, 1225–1242 (2020). doi:10.1038/s41418-019-0425-3

79. M. Roos, U. Pradère, R.P. Ngondo, A. Behera, S. Allegrini, G. Civenni, J.A. Zagalak, J.R. Marchand, M. Menzi, H. Towbin, J. Scheuermann, D. Neri, A. Caflisch, C.V. Catapano, C. Ciaudo, J. Hall, A Small-Molecule Inhibitor of Lin28. ACS Chem. Biol. **11**, 2773–2781 (2016). doi:10.1021/acschembio.6b00232

80. J. Balzeau, M.R. Menezes, S. Cao, J.P. Hagan, The LIN28/let-7 Pathway in Cancer, Front. Genet. 8, (2017) doi:10.3389/fgene.2017.00031

Figures

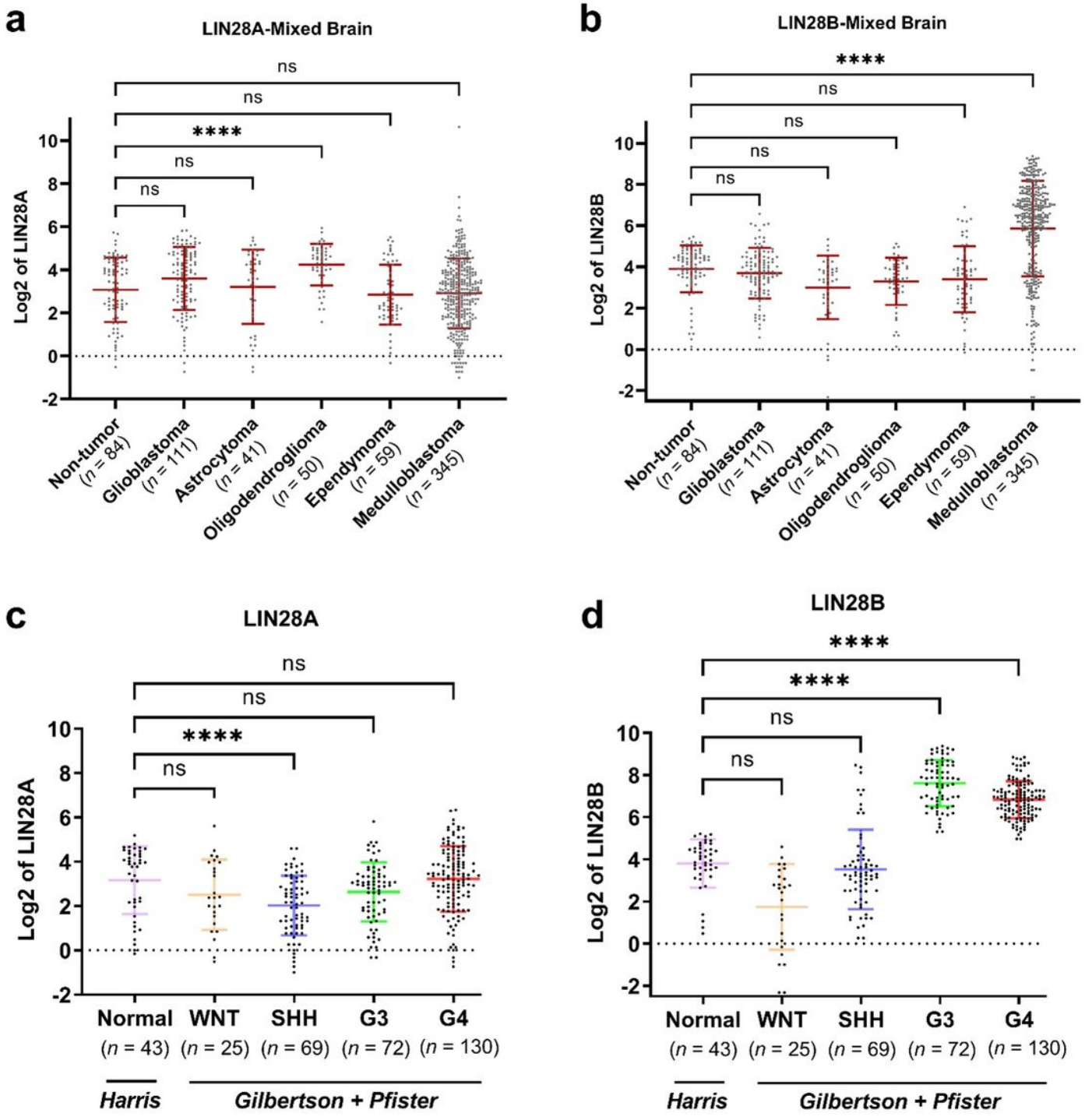

Figure 1

LIN28A and LIN28B expression in different brain tumours and normal brain tissue. **(a)** LIN28A and **(b)** LIN28B mRNA expression in MB (Donson [48], den Boer [49], Gilbertson [50] and Pfister [51, 52] datasets; n = 345) compared to non-tumour brain tissues (Harris [46], Sun [47], Donson and den Boer datasets; n = 84) and different brain tumours [Glioblastoma (Sun and Donson datasets; n = 111), Astrocytoma (Sun and Donson datasets; n = 41), Oligodendroglioma (Sun dataset, n = 50), and Ependymoma (Donson and den Boer dataset, n = 59)], (ns: not significant $p > 0.05$, **** $p < 0.0001$, non-parametric test, with Kruskal-Wallis test multiple comparisons, mean with SD, n = 690). **(c)** LIN28A and **(d)** LIN28B mRNA expression in different MB subgroups (Gilbertson and Pfister datasets; n = 296) and normal brain tissues (Harris dataset, n = 43), (ns: not significant $p > 0.05$, **** $p < 0.0001$, non-parametric test, with Kruskal-Wallis test multiple comparisons, mean with SD, n = 339)

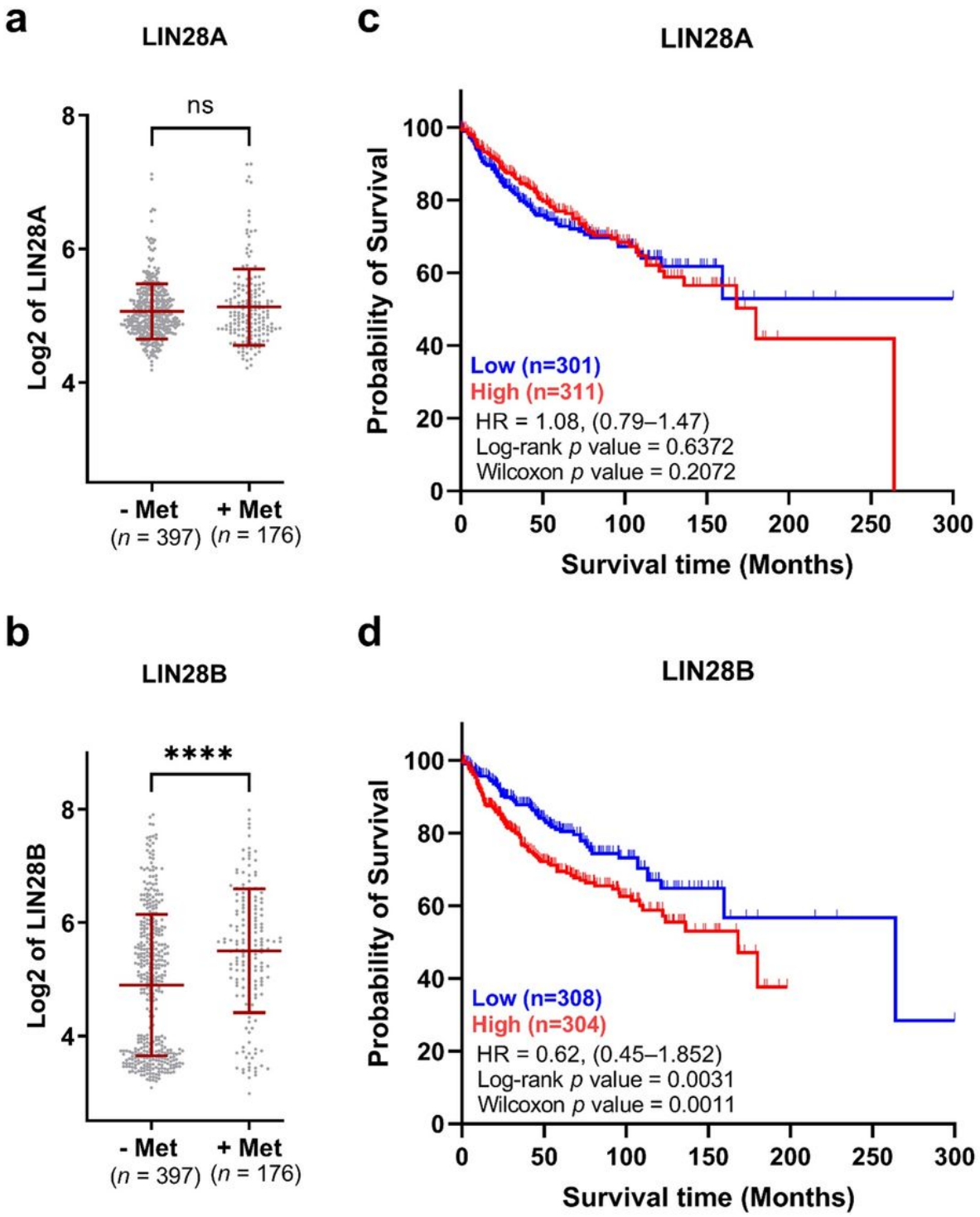

Figure 2

Stratification of MB metastatic status and overall patient survival based on LIN28A and LIN28B expression. (**a**) LIN28A and (**b**) LIN28B mRNA expression (log 2 transformed) present in Cavalli dataset [6] of MB non-metastatic patients (- Met, n = 397) versus MB metastatic patients (+ Met, n = 176). Data were exported from R2 Genomics software and plotted in GraphPad Prism. ns: not significant $p > 0.05$, **** $p < 0.0001$, two-tailed unpaired non-parametric *t*-test, with Mann-Whitney test for statistical

comparisons, mean with SD, n = 573). Kaplan–Meier curves demonstrate the association between (**c**) LIN28A and (**d**) LIN28B expression and overall patient survival present from the Cavalli dataset [6]. Data was extracted from GlioVis portal and plotted in GraphPad Prism. Blue: low expression, Red: high expression. Number of patients with high or low LIN28 expression are shown between brackets. HR: hazard ratios.

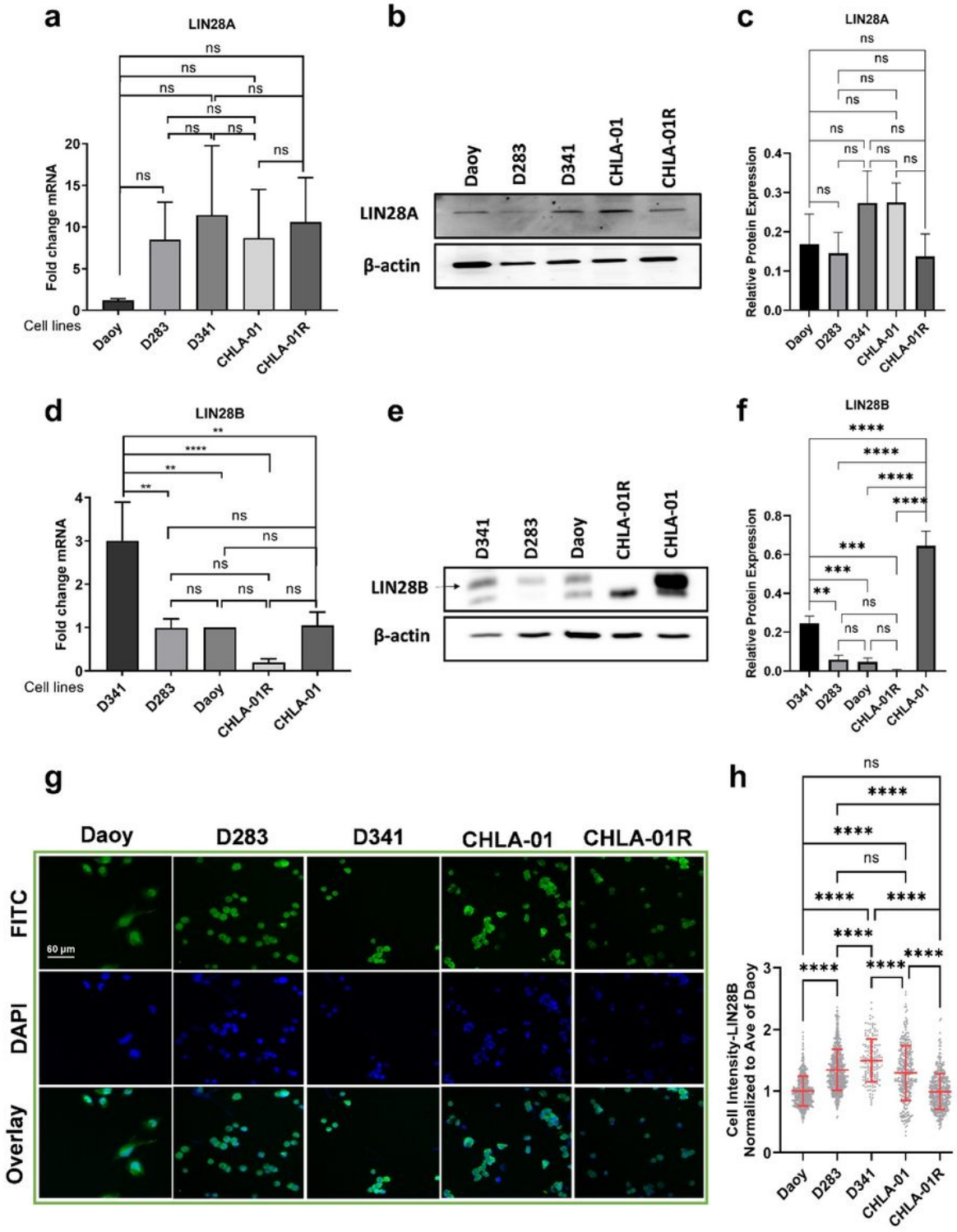

Figure 3

mRNA and protein expression of LIN28A and LIN28B in multiple MB cell lines. mRNA expression level of (**a**) LIN28A and (**d**) LIN28B. ns: not significant, $P > 0.05$, ** $P < 0.01$, **** $P < 0.0001$, one-way ANOVA, with Tukey's multiple comparisons, mean with SD). (**b**, **e**) Representative immunoblots of (b) LIN28A and (e) LIN28B proteins with β-actin as loading control. (**c**, **f**) Densitometry analysis of total (c) LIN28A and (f) LIN28B protein levels (normalized to β-actin as loading control) in D341, D283, Daoy, CHLA-01R-MED, and CHLA-01-MED MB cell lines. ns: not significant $p > 0.05$, ** $p < 0.01$, *** $p < 0.001$, **** $p < 0.0001$, one-way ANOVA, with Tukey's multiple comparisons. Each bar shows mean ± SD from three independent experiments (three biological replicates). (**g**) Representative immunofluorescence images of different MB cells marked with antibody against LIN28B (FITC; Green) and DAPI DNA staining (blue). Scale bar, 60 μm. (**h**) Quantitative data of LIN28B protein expression intensity in Daoy (n = 554), D283 (n = 631), D341 (n = 150), CHLA-01 (n = 318) and CHLA-01R (n = 393) cells. Data represents mean ± SD from three independent experiments. ns: not significant, **** $p < 0.0001$, one-way ANOVA, with Tukey's multiple comparisons.

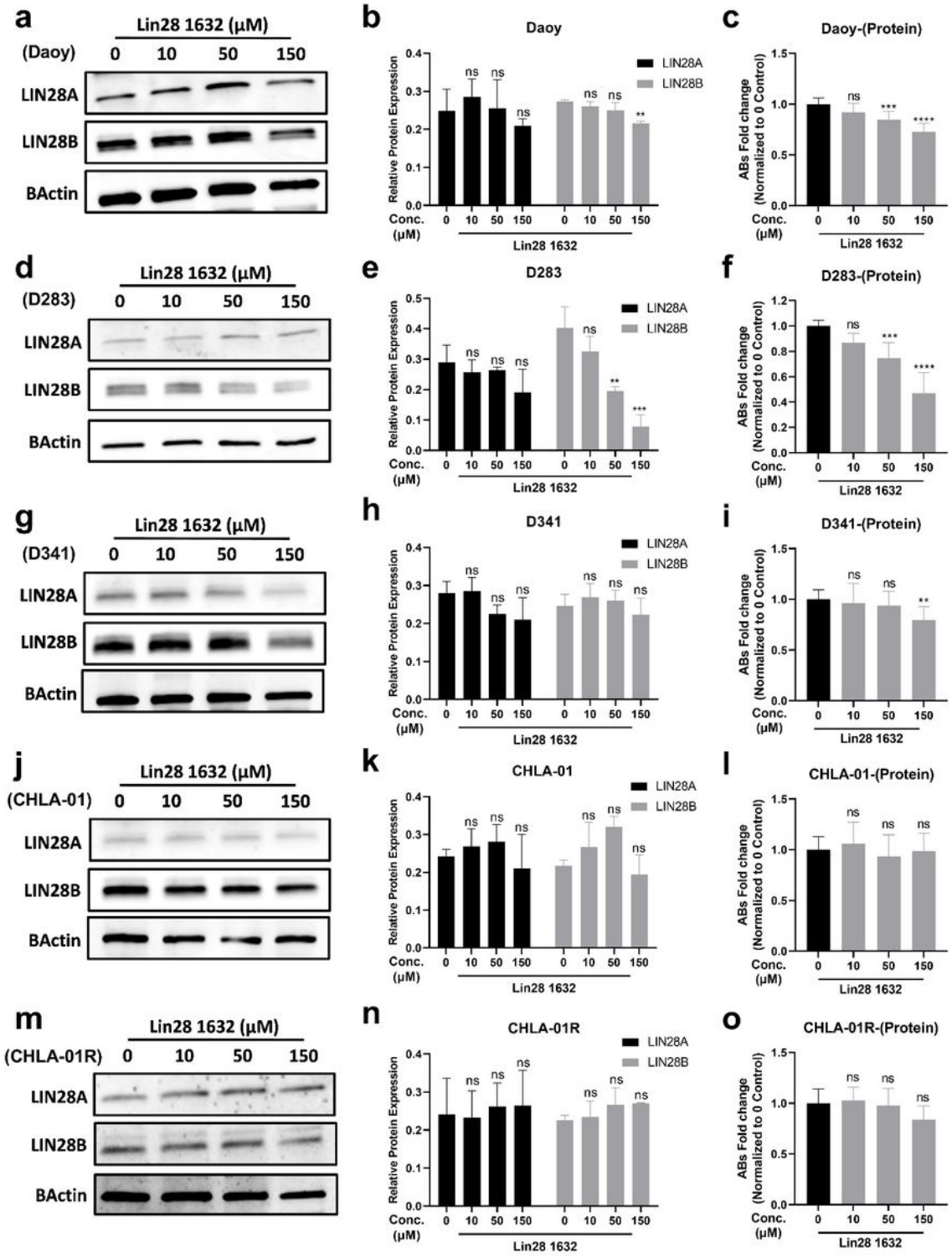

Figure 4

Effect of LIN28 inhibition on LIN28A and LIN28B protein expression levels and cell viability in MB cell lines. MB cells were treated with different concentrations of Lin28 1632 (0, 10, 50 and 150 μM) for 72 h. From left to right, each row represents: Representative immunoblots, densitometry analysis of total LIN28A and LIN28B protein levels (normalized to β-actin as loading control), and cell protein content in five different MB cell lines; (**a-c**) Daoy, (**d-f**) D283, (**g-i**) D341, (**j-l**) CHLA-01-MED, and (**m-o**) CHLA-01R-MED

cells. Each bar shows mean ± SD from three independent experiments (three biological replicates). Relative protein expression represents relative LIN28A and/or LIN28B expression quantity in total protein bands intensity after β-actin normalization. (ns: not significant $p > 0.05$, ** $p < 0.01$, *** $p < 0.001$, **** $p < 0.0001$, one-way ANOVA, with Tukey's multiple comparisons).

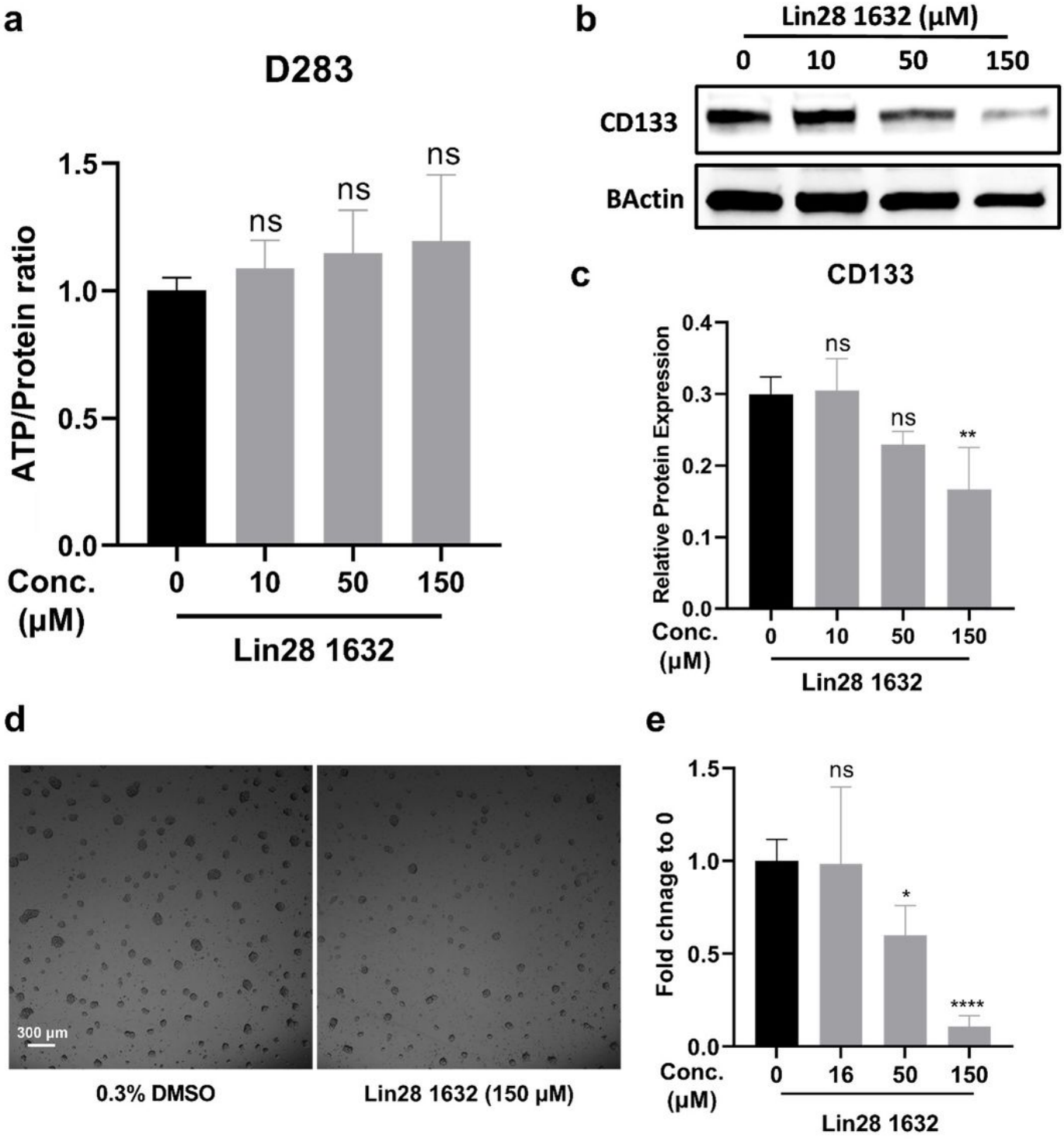

Figure 5

Effect of Lin28 1632 on CD133 protein expression in D283 Cells and on the sphere formation of CHLA-01R cells. (**a**) Intracellular ATP levels normalized to protein content in D283 cells. (ns: not significant). (**b**) Representative immunoblot of CD133 and β-actin proteins in D283 cells treated with Lin28 1632 (0-150 μM). (**c**) Densitometric analysis of relative CD133 protein levels (normalized to β-actin as loading control) in D283 cells. (ns: not significant $p > 0.05$, ** $p < 0.01$, one-way ANOVA, with Tukey's multiple comparisons). Bars represent mean ± S.D. from three independent experiments (three biological replicates). (**d**) Representative images of 3D spheroids. Scale bar, 300 μm. (**e**) Concentration-dependent response of Lin28 1632 on sphere size and number. Spheres size and numbers were quantified for all acquired images using ImageJ software. Results for each concentration were standardized to the non-treated control (0.3% DMSO) as fold change. Data expressed as mean ± SD from three independent repeats with three replicates each. (ns: not significant $p > 0.05$, * $p < 0.05$, *** $p < 0.001$, one-way ANOVA, with Tukey's multiple comparisons).

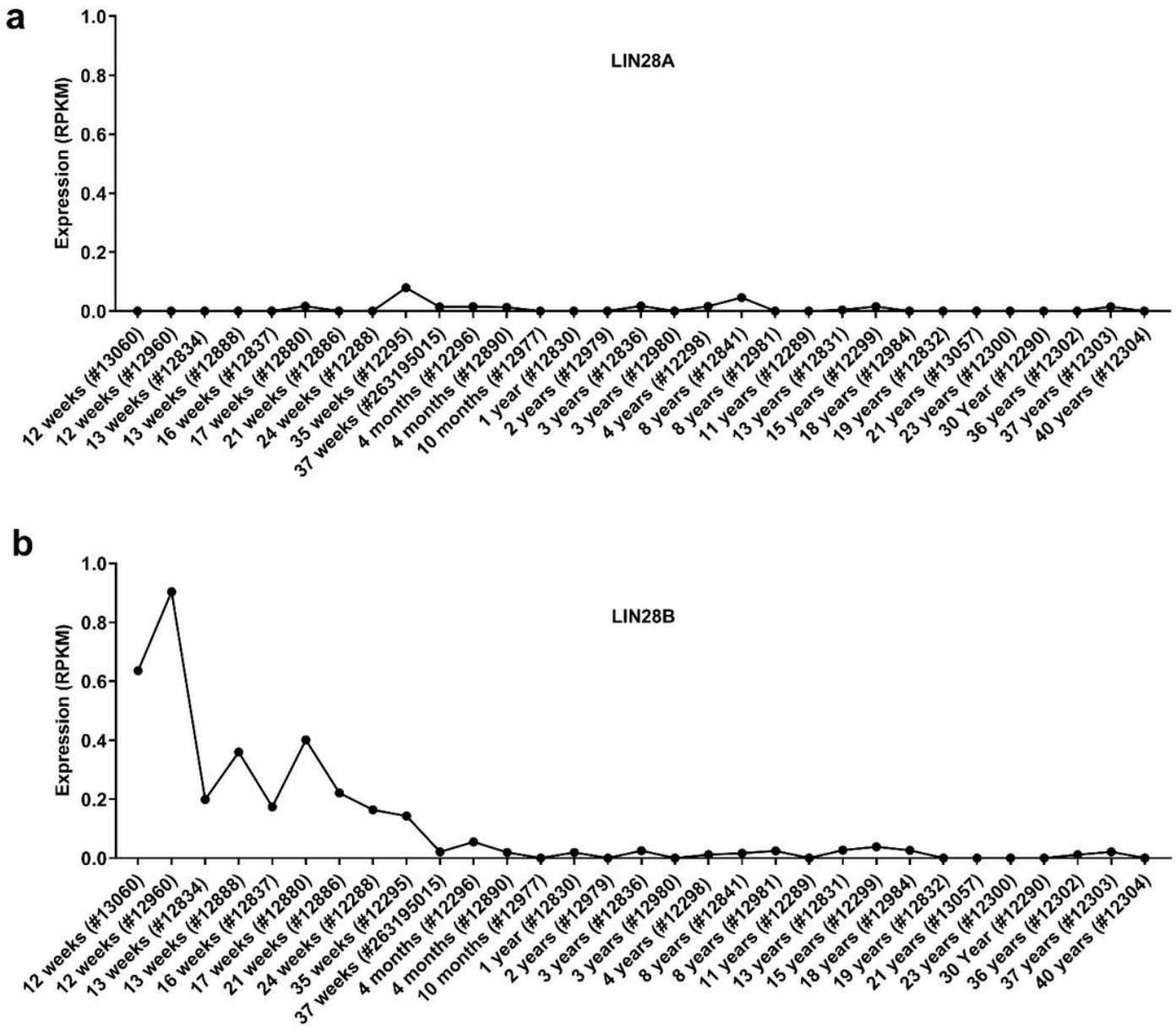

Figure 6

Age-dependent cerebellar LIN28 expression. Microarray data of the cerebellum of the developing brain were obtained from the BrainSpan Atlas of the Developing Human Brain (www.brainspan.org). A total of 31 cerebellum samples from 12 post-conceptual weeks to 40 years of age. Expression values of (**a**) LIN28A and (**b**) LIN28B are shown in reads per kilobase of transcript (RPKM). Donor ID for each sample is stated in the bracket.